sciendo DOI: 10.2478/ace-2018-0048 ARCHIVES OF CIVIL ENGINEERING
Vol. LXIV ISSUE 4 2018

© 2018 by K. Brzezińska, A. Szychowski. This is an open access article distributed under
the Creative Commons Attribution-NonCommercial-NoDerivs license (http://creativecommons.org/licenses/by-nc-nd/3.0/)

STABILITY AND RESISTANCE OF STEEL CONTINUOUS BEAMS WITH THIN-WALLED BOX SECTIONS

K. BRZEZIŃSKA[1], A. SZYCHOWSKI[2]

The issues of local stability and ultimate resistance of a continuous beam with thin-walled box section (Class 4) were reduced to the analysis of the local buckling of bilaterally elastically restrained internal plate of the compression flange at longitudinal stress variation. Critical stress of the local buckling was determined using the so-called Critical Plate Method (CPM). In the method, the effect of the elastic restraint of the component walls of the bar section and the effect of longitudinal stress variation that results from varying distribution of bending moments were taken into account. On that basis, appropriate effective characteristics of reliable sections were determined. Additionally, ultimate resistances of those sections were estimated. The impact of longitudinal stress variation and of the degree of elastic restraint of longitudinal edges on, respectively, the local buckling of compression flanges in the span section (*p*) and support section (*s*) was analysed. The influence of the span length of the continuous beam and of the relative plate slenderness of the compression flange on the critical ultimate resistance of box sections was examined.

Keywords: thin-walled elements, box sections, continuous beam, local critical resistance, design ultimate resistance

1. INTRODUCTION

Metal thin-walled elements (with Class 4 section) are commonly used in modern metal construction as, e.g. load carrying elements of roof purlins [11] or wall girts. Cold-formed open sections (e.g. Z-, C- or sigma sections), and also box sections are often employed. For light framing systems, GEP sections provide an interesting solution [8]. As regards the occurrence of instability phenomena,

[1] MSc., Eng., Kielce University of Technology, Faculty of Civil Engineering, Al. Tysiąclecia PP 7, 25-314 Kielce, Poland, e-mail: k.brzezinska@tu.kielce.pl
[2] DSc., PhD., Eng., Kielce University of Technology, Faculty of Civil Engineering, Al. Tysiąclecia PP 7, 25-314 Kielce, Poland, e-mail: aszychow@tu.kielce.pl

purlins with open section can undergo local buckling, distortional buckling, lateral torsional buckling about a forced rotation axis, which can be caused by, e.g. wind suction, or gravitational loads in near-support segments of continuous beams. That results from the fact that thin-walled open sections have low wall stiffness both in local buckling and distortional buckling, and also low stiffness of the whole section in torsion.

By contrast, thin-walled box sections are far less susceptible to local buckling because in the section only internal walls are found. They are more resistant to local buckling compared with cantilever walls [16], or cantilever walls with edge stiffener that are prone to distortional buckling [17]. Additionally, box sections are virtually insensitive to distortional buckling, and in majority of cases, are resistant to lateral torsional buckling. In study [3], the so-called deformability buckling was discussed, however that can occur only at compressive stress level that substantially exceeds the critical stress of local buckling. The resistance of box sections results from substantial torsional stiffness of hollow structural sections. Additionally, due to advantageous longitudinal distribution of bending moments, with continuous beam systems, it is possible to utilise the effect of longitudinal stress variation in the local stability analysis [12].

As regards thin-walled elements in bending, it is necessary to account for the possibility of occurrence of the local buckling of the compression flange, and also of webs in bending and shear.

In order to determine the resistance of thin-walled section, the effective width method is commonly used. Basically, the method involves the determination of the critical stress of local buckling (σ_{cr}^{L}) for individual walls of the section. The assumptions that are made concern the wall pin support, and constant longitudinal stress distribution. On the basis of the above, relative plate slenderness $\lambda_p=\sqrt{fy/\sigma_{cr}^{L}}$ and the wall effective width $b_{eff}=\rho(\lambda_p)b$ are determined.

This study is concerned with the determination of the resistance of a continuous beam (e.g. purlin) with thin-walled box section. In the procedure, the following are taken into account: 1) the effect of the weakest wall elastic restraint in the stiffening walls, and 2) effect of longitudinal stress variation caused by variation in bending moments.

In the analysis, it was assumed that the box section was constant over the whole beam length (Fig.1). Here, the end span is decisive for the continuous beam resistance. The case when the first (end) span is additionally strengthened, and intermediate spans decide the resistance will be analysed in a separate study.

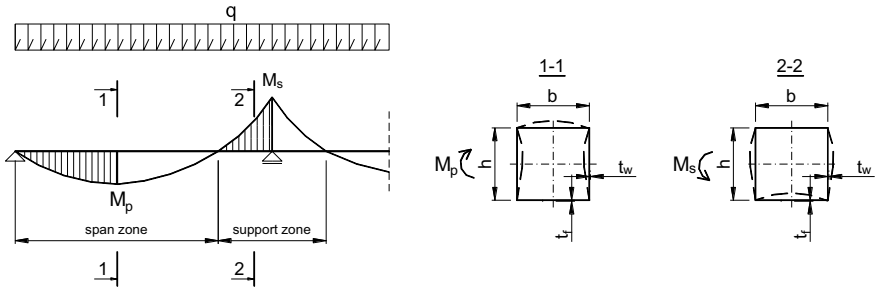

Fig. 1. Static model of the end span of continuous beam with thin-walled box section

2. COMPUTATIONAL MODEL OF LOCAL BUCKLING

In the computations of the local stability of thin-walled metal elements in accordance with the European standards EC-3 [16–18], a concept was assumed that component plates (walls) of the section are pin-supported on longitudinal edges of their connection. For the plates separated in this manner critical stress is determined for each of them individually. In accordance with this approach, the local critical resistance of the section, determined from the local buckling condition, depends on the critical stress of the weakest plate. The standard [17] Chapter 5.3 (Table 5.2) allows modelling the walls with rotational and translational spring stiffeners, however, it does not provide any solutions that concern local buckling. In this respect, it is recommended that the designer should rely on the computational model acc. the code [16]. That is equivalent to adopting a concept of separation of simply supported plates. After determining relative slenderness of individual walls, the respective widths are estimated. Then, they are put together to make an effective cross-section. Additionally, in design calculations, the effect of longitudinal stress variation is disregarded, although it is often found to occur in practice.

The effect of longitudinal stress variation in pin-supported internal wall in compression was taken into account, among others, in [2, 6, and 15]. A more accurate computational model that takes into account the impact of local buckling on the resistance of thin-walled sections was presented in study [12]. The Critical Plate Method (CPM) reported in the study accounts for both the effect of the elastic restraint of component walls, and also that of longitudinal stress variation.

3. LOCAL CRITICAL RESISTANCE AND DESIGN ULTIMATE RESISTANCE OF THE SECTION

In study [12], a concept of the local critical moment (M_{cr}^{L}) of thin-walled section was developed. It is determined from the condition of the local buckling of the bar segment under simple loading pattern (M). The local critical resistance of the section in bending can be interpreted as resistance in the pre-buckling behaviour. also constitutes a limit to the validity of the theory on thin-walled bars with a rigid cross-section contour.

In study [5], resistance of thin-walled section from the condition of yield of the most compressed edge of the effective cross-section (conservative estimation of the ultimate resistance) was differentiated from the section resistance at the failure stage, associated with the kinematically admissible mechanism of plastic hinge (non-conservative estimation of ultimate resistance). For structural designers, the so-called design resistance determined from the condition of yield of the most compressed edge of the effective cross-section, i.e. conservative estimation of the ultimate resistance, is of key importance. Conversely, resistance at the failure stage is used in the design of mechanical energy absorbers [5].

Consequently, in study [12], resistance from the condition of yield of the most compressed edge of the effective section (i.e. conservative estimation of the ultimate resistance acc. [5]) was specified as the design ultimate resistance.

4. THE CONCEPT OF THE CRITICAL PLATE METHOD (CPM) ACC. [12]

As regards thin-walled sections, the application of the CPM method involves primarily the identification of the critical plate (CP), which is decisive for local buckling under a given stress state. Then, it is assumed that CP longitudinal edges are elastically restrained against rotation in the neighbouring restraining plate (RP), or in the neighbouring restraining plates (RPs), e.g. in the webs. That means that for CP, the critical stress is higher than when it is assumed the plate is simply supported. The index of CP elastic restraint in RP is determined from formula:

$$\kappa = 1/(1 + 2D_s / b_s C_\theta) \tag{4.1}$$

where: C_θ - rotational spring stiffness equal to the bending moment created by rotation by a unit angle ($C_\theta = M/\theta$), b_s – width of the plate subjected to buckling (CP), D_s - plate flexural rigidity acc. formula:

(4.2) $$D_s = \frac{Et_s^3}{12(1-\nu^2)}$$

where for E=210000 N/mm^2 and ν=0.3, it can be approximately assumed that D_s=19200 t_s^3.

The critical stress, determined after taking into account the effect of elastic restraint and longitudinal stress variation (in accordance with linear or non-linear functions), is utilised to: 1) determine the local critical resistance of the section [12], 2) specify the effective widths of individual walls, 3) determine the design ultimate resistance [12].

For thin-walled box sections, the CPM assumptions are as follows: 1) CP acts as an internal plate, bilaterally elastically restrained against rotation, 2) CP to RP connection is rigid (i.e., on the longitudinal edge of their connection, the conditions of continuity of displacements – rotation angles, and forces - bending moments, are met), 3) the transverse edges of the plates (CP and RP) are simply supported on the bar segment ends, 4) thin-walled bar segment, with the length of ls, is defined as follows: a) for constant longitudinal stress distribution – a distance between the so-called buckling nodal lines, b) for longitudinal stress variation - a distance between transvers stiffeners (diaphragms, ribs or supports) that maintain a rigid section contour, but not longer than the range of the compression zone in the critical plate [13]. The conditions under which assumption 2 can be adopted were discussed in [12].

5. ALGORITHM OF THE CPM METHOD FOR THIN-WALLED BOX SECTIONS UNDER UNIDIRECTIONAL BENDING

In transverse bending, for a majority of typical, cold-formed box sections [1], it is local buckling of the compression flange that decides, as a rule, their resistance. Because of their geometric topology, those sections were categorised as semi-complex group in study [12].

The ultimate h of the section, at which the compression flange buckling and web in-plane bending occur almost simultaneously can be given from formula [12]

(5.1) $$h_0 = \sqrt{\frac{k_w^0}{k_f^0}} \cdot \left(\frac{t_w b}{t_f} \right)$$

where: k^0_i - basic plate buckling coefficient for separate, simply supported i-th plate at given load distribution (k^0=4 for axial compression, k^0=23.9 for in-plane bending).

For $h<h_0$, it is the compression flange that decides local buckling, whereas for $h>h_0$, the weakest section wall, in the pre-buckling behaviour, is the web under in-plane bending.
The algorithm for determining the local critical resistance and the design ultimate resistance of the box section under bending is as follows:

1) Identification of CP for semi-complex section on the basis of condition:

(5.2) $$\sigma^0_{cr,s} = \min\{\sigma^0_{cr,i}\}$$

(5.3) $$\sigma^0_{cr,i} = k^0_i \sigma_{E,i}$$

where: $\sigma_{E,i}$ - Euler stress for the i-th plate.

It should be noted that for $h<2{,}44b(t_w/t_f)$, the compression flange is the critical plate, which directly results from dependence (3). The case of welded box sections with $h>h_0$, in which buckling of webs in bending and shear is decisive for the critical resistance will be analysed in a separate study.

2) Making assumption on the initial value of the index of fixity of CP edge (for the so-called zero step), e.g. κ_0 =0.3
3) Determination of the expected critical length (l_{cr}) for a single half-wave of CP buckling [12,14] acc. formula:

(5.4) $$l_{cr} = b_s\left(1 - 0.23\kappa + 0.07\kappa^{-2} - 0.17\kappa^{-3}\right)$$

4) Calculation of coefficient η [4,12], depending on the loading diagram and means of RP excitation (load M_1) due to CP undergoing buckling (Fig.2):

(5.5) $$\eta = \sqrt{33.4 + 50.7\left(b_r / l_{cr}\right)^2} - 2.78$$

where: b_r – RP width.

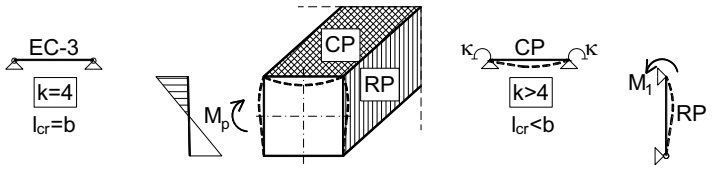

Fig. 2. Box section division into critical (CP) and restraining (RP) plates for $h<2{,}44b(t_w/t_f)$

5) Determination of σ_{cr} acc. formula:

(5.6) $$\sigma^{0}_{cr,s} = k^{*}\sigma_{E,s}$$

where: k^* – plate buckling coefficient for the more accurate computational model.

Coefficient k^* can be determined, acc. [14], from the following formulas:

a) for **linear** stress distribution (Fig. 3a):

(5.7) $$\begin{aligned} k^{*} = k_{\infty} + [&3{,}659m - 2{,}581m^2 + 1{,}184m^3 + (0{,}533m - 0{,}45m^2 + 0{,}218m^3)\kappa + \\ &(1{,}519m - 1{,}933m^2 + 1{,}046m^3)\kappa^3 - (2{,}536m - 4{,}247m^2 + 2{,}409m^3)\kappa^5 + \\ &(2{,}413m - 3{,}635m^2 + 1{,}992m^3)\kappa^7]/\gamma_s^{(0{,}68+0{,}04m)} \end{aligned}$$

b) for **non-linear** stress distribution (in accordance with 2° parabola, Fig.3b):

(5.8) $$\begin{aligned} k^{*} = k_{\infty} + [&3{,}814m - 6{,}58m^2 + 6{,}758m^3 - 2{,}572m^4 + (0{,}521m + \\ &- 1{,}307m^2 + 1{,}488m^3 - 0{,}59m^4)\kappa + (1{,}891m - 5{,}218m^2 + 6{,}174m^3 + \\ &- 2{,}529m^4)\kappa^3 - (4{,}555m - 14{,}648m^2 + 17{,}966m^3 - 7{,}454m^4)\kappa^5 + \\ &+ (3{,}833m - 11{,}694m^2 + 14{,}149m^3 - 5{,}833m^4)\kappa^7]/\gamma_s^{(1+0{,}04m)} \end{aligned}$$

where: $m = 1 - \sigma_1/\sigma_0$ - coefficient of the longitudinal stress distribution (Fig.3), $\gamma_s = l_s/b_s$

The plate buckling coefficient (k_∞) of the internal plate that is elastically restrained and indefinitely long [14], can be determined from the formula:

(5.9) $$k_{\infty} = 4 + 0{,}746\kappa + 2{,}304\kappa^3 - 2{,}836\kappa^5 + 2{,}73\kappa^7$$

Additionally, coefficients $k^* \approx k_{SN}$ can also be determined from formulas derived using neural networks as demonstrated in studies [9,10].

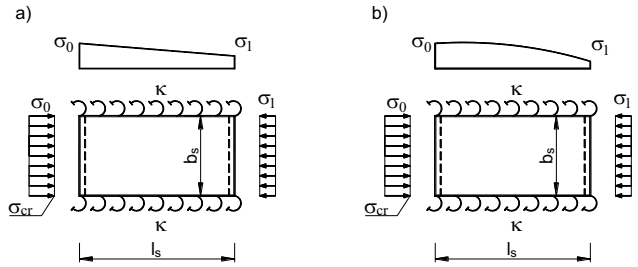

Fig. 3. Longitudinal stress distribution in the internal plate: a) linear, b) non-linear (acc. the second degree parabola)

6) Calculation of the critical stress $\sigma_{cr,r}$ for RP (with the width of b_r) under in-plane bending for one buckling half-wave of CP (l_{cr}) acc. section 3 [7].

(5.10) $$\sigma_{cr,r} = \frac{Et^2}{l_{cr}^2 b_r^4}(11{,}32 l_{cr}^4 + 1{,}97 b_r^4 + 12{,}06 l_{cr}^2 b_r^2)$$

7) Determination of the rotational spring stiffness C_θ acc. (13), and of the index of fixity $\kappa_{i=i+1}$ acc. (1) for the first (i=1) and successive iteration steps

(5.11) $$C_\theta = \frac{c_j \eta D_r}{b_r}\left(1 - \frac{\sigma_{cr,e}}{\sigma_{cr,r}}\right)$$

where: c_j - parameter of geometric configuration of the plates that are in contact on the j-th edge, for box section c_j=1 [12], D_r=19200 t_r^3 – flexural stiffness of RP.

8) Repetition of steps 3) to 7) until $\kappa_i \approx \kappa_{i+1}$

9) $\sigma_{cr,s}(\kappa_{i+1})$ acc. formula (8) is the sought critical stress for CP

10) Determination of the local critical resistance of the section in bending on the basis of the critical stress in CP acc. formula:

(5.12) $$M_{cr}^{L} = \sigma_{cr}^{L} W_{el,y} / \gamma_{M0}$$

where: $W_{el,y}=I_y/z_c$ – elastic section modulus of the gross cross-section.

11) Determination of the design ultimate resistance of the section acc. formula:

(5.13) $$M_{eff} = W_{eff} f_y / \gamma_{M0}$$

where: W_{eff} – section modulus of the effective cross-section.

For box section, section modulus W_{eff} is determined for the following assumptions [12]: a) plate slenderness of the compression flange (critical plate CP) should be determined on the basis of the critical stress that is determined while taking into account the effect of bilateral elastic restraint of the plate in the webs of the section, and also longitudinal stress variation, b) for webs (restraining plates RPs), simple support should be adopted on the same edges, c) boundary conditions on the second internal edge of RP generally produce only a slight effect on the results of computations, (in a conservative manner, simple support can also be assumed here), d) the effect of the potential longitudinal stress variation in RP is minimal and, therefore negligible, e) the widths determined in the manner above are put together to form an effective cross-section. The difference between the algorithm presented above and the classic version of the effective width method was discussed, in detail, in study [12].

6. EXAMPLE OF CPM APPLICATION TO THE DETERMINATION OF THE RESISTANCE OF THE CONTINUOUS BEAM UNDER TRANSVERSE BENDING

Computations were performed, among others, for five-span continuous beam (e.g. purlin) with the span length L=4m and thin-walled box section Sk250x250x4. The beam was made from S355 grade steel, and the continuous load was uniformly distributed.

Beam structure and loading, graphs of bending moments and parameters adopted in the analysis are shown in Fig.4. The relationship between the maximum support moment M_s, and the maximum span moment M_p in the end span is $u=|M_s/M_p|=1.351$. In the support sections of the beam, external reinforcing ribs (diaphragms) were used. Their role is, among others, to transfer support reactions.

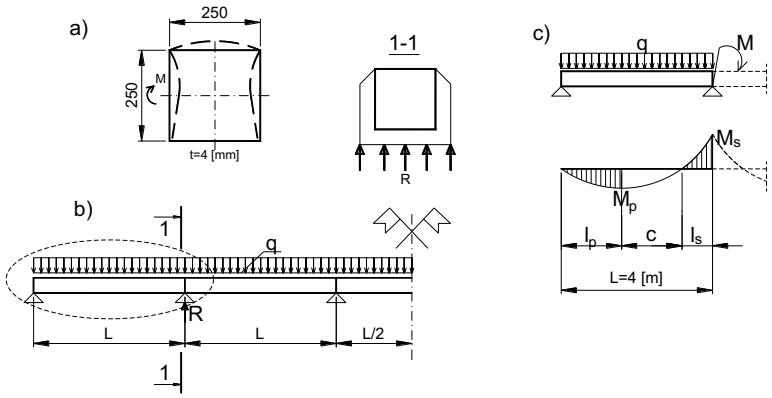

Fig. 4. Continuous beam structure and loading: a) box cross-section, b) load distribution, c) computational model acc.to CPM

For five-span continuous beam under uniform load, in the first (end) span, non-linear distribution of the bending moment M_y is found. The maximum values are (M_p and M_s), in addition, for the range (l_p+c) the M_y graph is convex, whereas for the range ls, it is concave. Such longitudinal distributions of M_y result in non-linear (along the beam length) distributions of normal stress (σ_x) that can cause local stability loss.

On the basis of the analysis of the results reported in study [6], it can be stated that as regards non-linear stress distribution for the whole span range (l_p+c), coefficient k takes essentially the same values as those determined for the reduced range l_p. For instance, for $\gamma_s \geq 2$, the differences do not exceed 1% and they decrease with the segment length. Conversely, in study [13], it was shown that if the sign of stress is changed, the design segment length can be limited to the compression zone range, as is the case in the support zone (l_s) of the continuous beam.

Consequently, from the standpoint of engineering calculations with the use of CPM, to determine the span section resistance, it is sufficient to assume a reliable length of the segment as l_p, and for the support section, a segment of the length l_s (Fig.5.). For the span segment, non-linear distribution M_y (in accordance with the second degree parabola) was assumed, whereas for the support segment, concave graph of M_y was conservatively approximated using linear distribution.

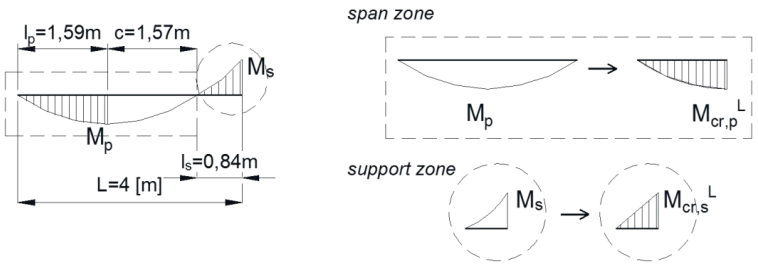

Fig. 5. Computational model of the end span of the continuous beam under uniformly distributed load

The results of computations of the local critical resistance for the reliable sections: span (p) and support (s), and of the critical resistance (q_{cr}) determined on that basis are listed in Table 1. The notations are as follows: $M_{cr,p}^{L}$, $M_{cr,s}^{L}$ represent local critical resistances of the span and support sections acc. CPM, and M_{cr}^{EC3} stands for the local critical resistance of an arbitrary section, determined on the basis of σ_{cr} computed acc. EC-3 [16]. In this case M_{cr}^{EC3} does not depend on the longitudinal distribution M_y, or the degree of the elastic restraint of the component walls of the section.

In row 1 of Table 1, the critical load value is given (q_{cr}), which results from the condition of reaching the local critical resistance of the support section $M_{cr,s}^{L}$, and in row 2 (q_{cr}), from $M_{cr,p}^{L}$ being reached in the span. Rows 3 and 4 of the same table show critical loads resulting from the condition of M_{cr}^{EC3} being reached in the support and span sections, respectively. In every case, the minimal critical load $q_{cr}^{\min}$ decides the critical resistance of the beam.

Table 1. Critical load (q_{cr})

	q_{cr} [kN/m]	M_p [kNm]	M_s [kNm]	q_{cr}^{min} [kN/m]	Local critical resistance [kNm]
1	60.13	74.94	**101.27**	**60.13**	$M_{cr,s}^{L}$ =**101.27**
2	69.87	**87.08**	117.68		$M_{cr,p}^{L}$ =**87.09**
3	37.91	47.25	**63.85**	**37.91**	M_{cr}^{EC3} =**63.85**
4	51.23	**63.85**	86.28		

The comparison of the results presented in Table 1 indicates that $M^{L}_{cr,s}$ is approx. 16% greater than $|M^{L}_{cr,p}|$. That results from different stress distributions and different lengths of the span (l_p) and support (l_s) segments. In spite of the fact that $|M^{L}_{cr,p}| < M^{L}_{cr,s}$, it is the near-support zone that decides the beam critical resistance, because: $u = 1{,}351 > |M^{L}_{cr,s} / M^{L}_{cr,p}| = 1{,}163$. Percentage increment in compared with is approx. 59%. The same relationship holds for the corresponding critical loads ($q^{\min}_{cr}$).

Table 2 shows the results of the design ultimate resistance for the reliable sections: span (p) and support (s), and of the critical loads (q_{eff}) determined on that basis. In Table 2, the symbols denote the following: $M^{CP}_{eff,p}, M^{CP}_{eff,s}$ - design ultimate resistances of the span and support sections acc. CPM, $M^{EC3}_{c,Rd}$ – design resistance of an arbitrary section acc. EC-3 [16,18]. In this case, $M^{EC3}_{c,Rd}$ does not depend on the longitudinal distribution M_y or the degree of elastic restraint of component walls.

In row 1 of Table 2, the value of the ultimate load (q_{eff}) is shown. It results from the condition of reaching the design ultimate resistance of the support section ($M^{CP}_{eff,s}$), and in row 2, (q_{eff}), from the condition of $M^{CP}_{eff,p}$ being reached in the span. Rows 3 and 4 of the table give the design loads from the condition of $M^{EC3}_{c,Rd}$ being reached in the support and span sections, respectively.

In every case, $q^{\min}_{eff}$ is decisive for the beam design ultimate resistance.

Table 2. Ultimate load (q_{eff})

	q_{eff} [kN/m]	M_p [kNm]	M_s [kNm]	q^{min}_{eff} [kN/m]	**Design ultimate resistance** [kNm]
1	57.35	71.48	**96.59**	**57.35**	$M^{CP}_{eff,s}$ =**96.59**
2	75.11	**93.62**	126.50		$M^{CP}_{eff,p}$ =**93.62**
3	52.13	64.97	**87.80**	**52.13**	$M^{EC3}_{c,Rd}$ =**87.79**
4	70.45	**87.81**	118.66		

The comparison of the results presented in Table 2 indicates that $M^{CP}_{eff,s}$ is approx. 3% greater than $|M^{CP}_{eff,p}|$. That results from different stress distributions and different lengths of the span (l_p) and

support (l_s) segments. Percentage increment in $M_{eff,s}^{CP}$ compared with $M_{c,Rd}^{EC3}$ is approx. 10%. The same relationship holds for the corresponding ultimate loads ($q_{eff}^{\min}$).

Figure 6. shows the effective sections of Sk250x250x4 profile determined for span and support sections, respectively acc. CPM (Fig.6. a, b) and acc. EC-3 (Fig.6. c, d). For instance, the effective width (b_{eff}) of the compression plate of the support section that decides beam resistance, acc. CPM is 16.5% greater than (b_{eff}) acc. EC-3. The shift of the neutral axis in the effective section acc. CPM compared with the gross section is e=9,2 mm. This value is lower, by 33%, than e=13.7 mm estimated acc. EC-3.

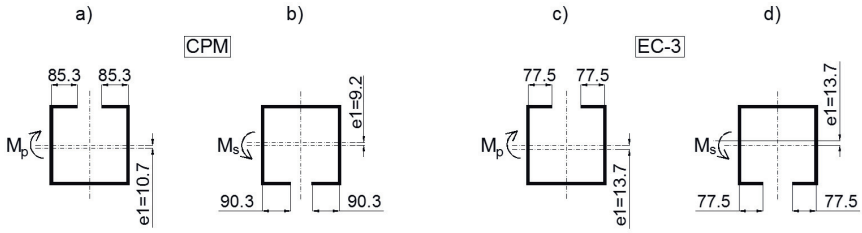

Fig. 6. Effective sections of Sk250x250x4 profile acc. CPM and EC-3

Table 3 shows the results of the analysis of the impact of the span length of the continuous beam of concern on the eigenvalue of M_{cr}^{L} and resistance M_{eff} computed acc. CPM and acc. EC-3 [16,18]. The comparison of the results indicates the following: 1) for the support segment that decides the resistance of the support segment structure (s), the percentage difference between the ultimate load q_{eff} obtained acc. CPM, compared with the value found in the code, stays at the level of approx. +10% for short spans (L=4m) and approx. 9% for longer spans (L=5;6;7m), 2) differences in resistances determined acc. CPM and EC-3 are inversely proportional to the length of spans, i.e. the shorter are the spans, the greater are the differences, 3) as the span length grows, the resistance parameters of the continuous beam are reduced.

Table 3. Comparison of CPM results and EC-3 calculations for four beam span lengths

		Sk250x250x4			
span length [m]	**L=**	**4**	**5**	**6**	**7**
slenderness	**l=b/t=**	62,5			
Euler stress [N/mm2]	$\sigma_{E,i}$=	48,64			
length of ranges [mm]	l_p=	1594	1992	2391	2789
	l_s=	842	1053	1263	1474
buckling coefficient	**for l_p: k*=**	5,46	5,41	5,38	5,35
	for l_s: k*=	6,34	6,18	6,06	5,97
critical stress acc. CPM [N/mm2]	**for l_p: $\sigma_{cr,s}$=**	265,37	263,03	261,47	260,37
	for l_s: $\sigma_{cr,s}$=	308,59	300,48	294,78	290,49
critical stress acc. EC3 [N/mm2]	$\sigma_{cr,0}$=	4 x 48,64 = 194,56			
local critical resistance [kNm]	**for l_p: $M_{cr,p}^{L}$=**	87,087	86,318	85,808	85,447
	for l_s: $M_{cr,s}^{L}$=	101,270	98,608	96,738	95,331
	Mcr^{EC3}=	63,848			
critical load acc. CPM [kN/m]	**for l_p: $q_{cr,p}^{CP}$=**	69,871	44,325	30,597	22,386
	for l_s: $q_{cr,s}^{CP}$=	**60,130**	**37,471**	**25,529**	**18,483**
critical load acc. EC3 [kN/m]	q_{cr}^{EC3}=	37,910	24,262	16,849	12,379
percentage increment of resistance [%]	q_{cr}^{CP} / q_{cr}^{EC3}	58,61	54,44	51,51	49,31
design ultimate resistance [kNm]	**for l_p: M_{eff}^{CP}=**	93,620	93,448	93,333	93,251
	for l_s: M_{eff}^{CP}=	96,591	96,061	95,681	95,392
	$M_{c,Rd}^{EC3}$=	87,787			
ultimate load acc. CPM [kN/m]	**for l_p: $q_{eff,p}^{CP}$=**	75,112	47,986	33,281	24,431
	for l_s: $q_{eff,s}^{CP}$=	**57,351**	**36,503**	**25,250**	**18,495**
ultimate load acc. EC3 [kN/m]	**for l_s: q_{eff}^{EC3}=**	52,130	33,354	23,169	17,020
percentage increment of resistance [%]	q_{eff}^{CP} / q_{eff}^{EC3}	10,02	9,44	8,98	8,67

Additionally, Table 3 also lists, for the sake of comparison critical and ultimate loads determined acc. CPM for the case, in which the span section was decisive for the beam resistance.

Table 4 shows the results of the analysis of the impact of slenderness on eigenvalue of M_{cr}^{L} and resistance M_{eff} of the continuous beam with the span length L=4m computed acc. CPM and EC-3. The comparison of the results indicates that: 1) with a reduction in the thickness of the section walls,

the values of the local critical resistance M_{cr}^{L} and of the critical load q_{cr} decrease, 2) the difference between the resistance results obtained acc. CPM and EC-3 is approx.+59%, 3) as thickness of the section wall decreases, the design ultimate resistance M_{eff} and the critical ultimate load q_{eff} are reduced, 4) the difference between the results produced acc. CPM and EC-3 is approx. +10% for t=3;4;5mm and approx. +8% for t=2mm.

Table 4. Comparison of CPM results and EC-3 calculations for four section wall thicknesses

		Sk250x250xt			
wall thickness [mm]	**t=**	**5**	**4**	**3**	**2**
slenderness	**l=b/t=**	50,0	62,5	83,3	125,0
Euler stress [N/mm2]	**$\sigma_{E,i}$=**	76	48,64	27,36	12,16
buckling coefficient	**for l_p: k*=**	5,46	5,46	5,46	5,46
	for l_s: k*=	6,34	6,34	6,34	6,34
critical stress acc. CPM [N/mm2]	**for l_p: $\sigma_{cr,s}$=**	414,64	265,37	149,27	66,34
	for l_s: $\sigma_{cr,s}$=	482,18	308,59	173,58	77,15
critical stress acc. EC3 [N/mm2]	**$\sigma_{cr,0}$=**	304,00	194,56	109,44	48,64
local critical resistance [kNm]	**for l_p: $M_{cr,p}^{L}$=**	169,449	87,087	36,881	10,970
	for l_s: $M_{cr,s}^{L}$=	197,046	101,270	42,888	12,757
	Mcr^{EC3}=	124,233	63,848	27,039	8,043
critical load acc. CPM [kN/m]	**for l_p: $q_{cr,p}^{CP}$=**	135,951	69,871	29,590	8,801
	for l_s: $q_{cr,s}^{CP}$=	**116,997**	**60,130**	**25,465**	**7,574**
critical load acc. EC3 [kN/m]	**q_{cr}^{EC3}=**	73,764	37,910	16,055	4,775
percentage increment of resistance [%]	**q_{cr}^{CP} / q_{cr}^{EC3}**	58,61			
design ultimate resistance [kNm]	**for l_p: M_{eff}^{CP}=**	127,409	93,620	62,796	36,116
	for l_s: M_{eff}^{CP}=	131,268	96,591	64,751	37,112
	$M_{c,Rd}^{EC3}$=	119,584	87,787	59,046	34,24
ultimate load acc. CPM [kN/m]	**for l_p: $q_{eff,p}^{CP}$=**	102,221	75,112	50,382	28,976
	for l_s: $q_{eff,s}^{CP}$=	**77,941**	**57,351**	**38,446**	**22,036**
ultimate load acc. EC3 [kN/m]	**for l_s: q_{eff}^{EC3}=**	71,003	52,124	35,059	20,332
percentage increment of resistance [%]	**q_{eff}^{CP} / q_{eff}^{EC3}**	9,77	10,03	9,66	8,38

It should be added that for the sake of comparison, Table 4 also gives the critical and ultimate load determined acc. CPM for the case, in which span section decided the beam resistance.

Figure 7 shows the critical resistance $M_{cr,s}$ (a) and critical load q_{cr} (b) as a function of slenderness λ_{CP}. The solid line represents the results acc. CPM, whereas the broken line those acc. EC-3.

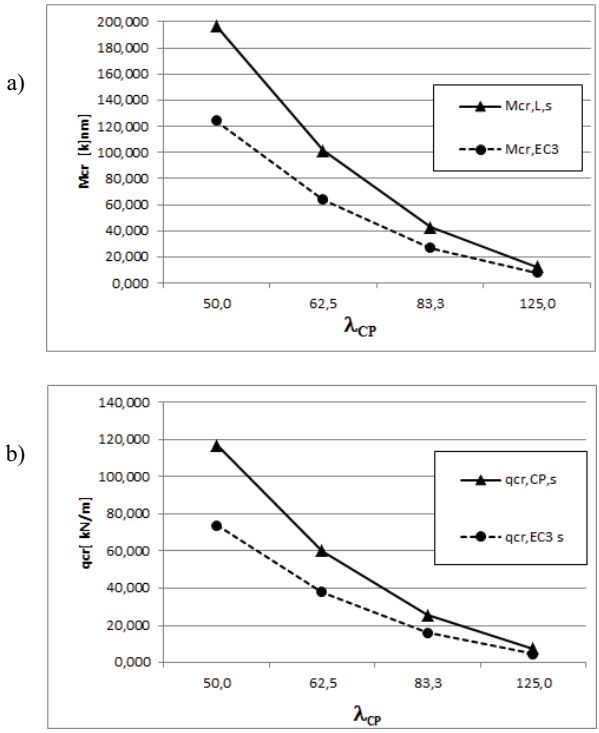

Fig. 7. Graphs of a) $M_{cr,s}$ and b) q_{cr} as a function of slenderness λ_{CP}

In Fig.8, the design ultimate resistance M_{eff} (a) and ultimate load q_{eff} (b) are shown as a function of slenderness λ_{CP}. The solid line represents the results acc. CPM, whereas the broken line those acc. EC-3.

a)

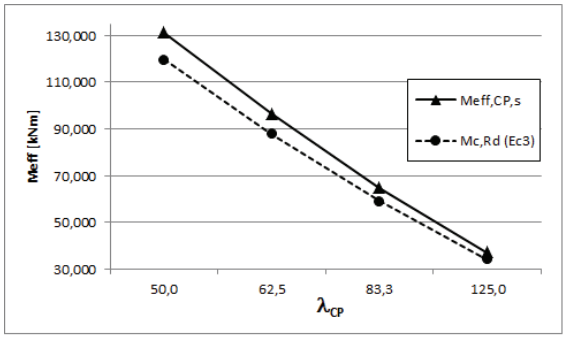

b)

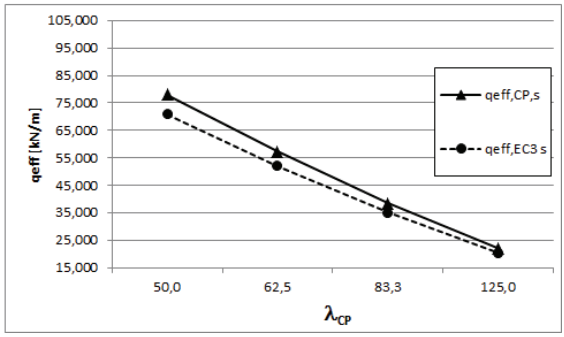

Fig. 8. Graphs of a) M_{eff} and b) q_{eff} as a function of slenderness λ_{CP}.

The analysis of the results (Tables 3,4, Figs.7,8) shows it is possible to state that in the example under consideration an approx. 59% increase in the continuous beam critical resistance, determined acc. CPM, translated into almost 10% increase in the design ultimate resistance when compared with computations acc. EC-3. This relationship does not depend on CP slenderness.

8. SUMMARY

The study shows the application of the Critical Plate Method (CPM) [12] to the determination of the local critical resistance (M_{cr}) and design ultimate resistance (M_{eff}) of thin-walled box section. The method accounts for the effect of the elastic restraint of component plates and longitudinal stress variation. The computations were performed for a more accurate model of behaviour of the internal critical plate (CP) and restraining plates (RPs) rigidly connected to CP. The local critical resistance determined in this way specifies the range of pre-buckling behaviour of the section and constitutes a limit to the validity of the theory on thin-walled bars with a rigid cross-section contour.

On the basis of the results presented Tables 1 and 2, it can be stated that the intermediate support segment (M_s) of the first span decides the resistance of five-span beam with thin-walled box section. The segment mentioned above is the first one, in which first the local critical resistance, and then design ultimate resistance are reached.

To determine the design ultimate resistance of the box section, the effective width method can be used. The method is applied to individual plates (Chapter 5 step 11), which follows the concept developed in study [12]. The relative slenderness values are determined on the basis of appropriate critical stress of the component plates. For CP, stress computations account for fixity indices and longitudinal stress variation. For RP, simple support conditions on the same edge and constant stress distribution along the length can be assumed. Such assumptions ensure calculations that are accurate enough from the technical standpoint for this class of thin-walled structures.

For the beam analysed in the example, made from cold-formed Sk250x250x4 box section and computed acc. CPM, approx. 59% increase in the critical resistance was found. That led to almost 10% increase in the design ultimate resistance when compared with the computational results obtained acc. EC-3.

As a result, the application of the more accurate computational model makes it possible to design thin-walled structures in a more optimal way. In the model, the unknown reserves of resistance are substituted with objective measures of reliability.

REFERENCES

1. W. Bogucki, M. Żyburtowicz: Tables for the design of metal structures (in Polish), 7th ed.,
2. P. S. Bulson: The stability of Flat Plates. Chatto and Windus, 1970.
3. A. Chudzikiewicz: General theory of thin-walled bars stability taking into account the cross-section deformability. Part II: Complex cross-sections bars (in Polish). Rozprawy Inżynierskie, Vol. VIII, 1960, Series 4, 805-841.
4. V. Kalyanaraman: Local buckling of cold-formed steel members. Journal of the Structural Division, vol. 105, pp. 813–828, 1979.
5. M. Kotełko: Thin-walled structures resistance and failure mechanisms (in Polish), Warsaw 2011.
6. Z. Kowal: The stability of compressed flange of plate girder with a box section (in Polish) Zeszyty Naukowe Politechniki Wrocławskiej, Budownictwo 1965, pp. 73–85.
7. L. Li, J. K. Chen: An analytical model for analyzing distortional buckling of cold-formed steel sections. Thin Walled Structures 46 (2008), pp. 1430–1436.
8. A. Łukowicz, E. Urbańska-Galewska, M. Gordziej-Zagórowska: Experimental testing of innovative cold-formed "GEB" section. Civil and Environmental Engineering Reports, pp. 129–140, 2015.
9. B. Potrzeszcz-Sut, A. Szychowski: Neural prediction of the buckling coefficient of the internal wall of the thin-walled element (in Polish), in: Konstrukcje Betonowe i Metalowe, pp. 259–266.
10. B. Potrzeszcz-Sut, A. Szychowski: Neural approximation of the buckling coefficient of compression flange of box girder evenly loaded transversely. Applied Mechanics and Materials, pp. 137–144, 2015.
11. K. Rzeszut, Ł. Polus: Numerical analysis of thin-walled purlins restrained by sheeting in elevated temperature conditions. Archives of Civil Engineering, vol. LXI, Issue 4, pp. 35–44, 2015.
12. A. Szychowski: Computation of thin-walled cross-section resistance to local buckling with the use of the Critical Plate Method. Archives of Civil Engineering, vol. 62, Series: 2, pp. 229–264, 2016.

13. A. Szychowski: Stability of cantilever walls of steel thin-walled bars with open cross-section. Thin-Walled Structures, pp. 348–358.
14. A. Szychowski: Buckling of internal walls in thin-walled members, Kielce-Suchedniów 2014, pp. 81–84.
15. C. Yu, B. W. Schafer: Effect of longitudinal stress gradients on elastic buckling of thin plates. J Eng Mech ASCE 2007, pp. 452–63.
16. PN-EN 1993-1-5:2006 Eurocode 3 - Design of steel structures - Part 1-5: Plated structural elements.
17. PN-EN 1993-1-3:2006 Eurocode 3 - Design of steel structures - Part 1-3: General rules. Supplementary rules for cold-formed members and sheeting.
18. PN-EN 1993-1-1:2006 Eurocode 3: Design of steel structures - Part 1-1: General rules and rules for buildings.

LIST OF FIGURES AND TABLES:

STATECZNOŚĆ I NOŚNOŚĆ STALOWYCH BELEK CIĄGŁYCH O SMUKŁOŚCIENNYCH PRZEKROJACH SKRZYNKOWYCH

Słowa kluczowe: elementy smukłościenne, przekroje skrzynkowe, belka ciągła, „lokalna" nośność krytyczna, obliczeniowa nośność graniczna

STRESZCZENIE:

Metalowe elementy cienkościenne o przekroju klasy 4. są powszechnie stosowane we współczesnym budownictwie metalowym, np. jako elementy nośne płatwi dachowych lub rygli obudowy ściennej. Stosuje się tutaj zarówno gięte na zimno przekroje otwarte (np. przekroje zetowe, ceowe lub sigma) jak również przekroje skrzynkowe.

W celu wyznaczenia nośności przekroju cienkościennego, powszechnie stosuje się metodę szerokości efektywnej. W ujęciu elementarnym polega ona na wyznaczeniu naprężeń krytycznych wyboczenia lokalnego (σ_{cr}^{L}), dla poszczególnych ścianek przekroju, przy założeniu podparcia przegubowego oraz stałego rozkładu naprężeń w kierunku podłużnym. Na tej podstawie wyznacza się płytową smukłość względną $\lambda_p=\sqrt{f_y/\sigma_{cr}^{L}}$ oraz szerokość efektywną ścianki $b_{eff}=\rho(\lambda_p)b$.

Stosowane aktualnie metody projektowania elementów cienkościennych zmierzają do uwzględnienia szeregu parametrów poprawiających odwzorowanie rzeczywistego zachowania się elementu cienkościennego w modelu obliczeniowym. W przypadku przekrojów kl. 4. do istotnych parametrów wpływających na nośność należą: 1) stopień sprężystego zamocowania płyt (ścianek) składowych przekroju pręta oraz, 2) współczynnik wzdłużnego rozkładu naprężeń.

W niniejszej pracy zajęto się wyznaczeniem nośności belki ciągłej o cienkościennym przekroju skrzynkowym z uwzględnieniem dokładniejszego modelu obliczeniowego. Wzięto pod uwagę zarówno efekt sprężystego zamocowania ścianki najsłabszej (płyty krytycznej CP) w ściankach usztywniających (płytach usztywniających RPs) jak również wzdłużną zmienność naprężeń wywołaną zmiennością momentów zginających. Do analizy przyjęto sytuację stałego przekroju skrzynkowego na całej długości belki. W takim przypadku, o nośności belki ciągłej decyduje skrajne przęsło.

Zagadnienie stateczności lokalnej i nośności granicznej belki ciągłej sprowadzono do analizy wyboczenia lokalnego obustronnie sprężyście zamocowanej płyty przęsłowej pasa ściskanego przy występowaniu wzdłużnej zmienności naprężeń. Naprężenia krytyczne wyboczenia lokalnego wyznaczono metodą płyty krytycznej (Critical Plate Method „CPM" [12]), w której uwzględniono efekt sprężystego zamocowania ścianek składowych przekroju pręta oraz efekt wzdłużnej zmienności naprężeń. Na tej podstawie wyznaczono „lokalną" nośność krytyczną (M_{cr}^{L}), określającą zakres dokrytycznego zachowania się przekroju (stanowiącą granicę ważności technicznej teorii prętów cienkościennych o sztywnym konturze) oraz odpowiednie charakterystyki efektywne miarodajnych przekrojów (przęsłowego i podporowego). Nośności graniczne (M_{eff}) przekrojów oszacowano metodą szerokości efektywnej przy następujących założeniach [12]: a) smukłość płytową pasa ściskanego (płyty krytycznej CP) wyznaczono na podstawie naprężeń krytycznych obliczonych z uwzględnieniem efektu obustronnego sprężystego zamocowania płyty w środnikach przekroju oraz przy uwzględnieniu wzdłużnej zmienności naprężeń, b) dla środników (płyt usztywniających RPs), na tych samych krawędziach przyjęto podparcie przegubowe, c) warunki brzegowe na drugiej krawędzi przęsłowej RP mają na ogół nieznaczny wpływ na wynik obliczeń, (konserwatywnie można tu również przyjąć podparcie przegubowe), d) wpływ ewentualnej wzdłużnej zmienności naprężeń w RP jest nieznaczny i można go pominąć, e) tak wyznaczone szerokości współpracujące „złożono" w efektywny przekrój poprzeczny. Takie założenia pozwoliły na technicznie wystarczająco dokładne obliczenie nośności tej klasy elementów cienkościennych

Ponadto w pracy przeanalizowano wpływ rozpiętości przęsła belki ciągłej oraz wpływ względnej smukłości płytowej pasa ściskanego na nośność krytyczną i graniczną przekrojów skrzynkowych. Na podstawie wyników zamieszczonych w tabelach 1 i 2 można stwierdzić, że przekrojem decydującym o nośności 5-cio przęsłowej belki o cienkościennym przekroju skrzynkowym jest pośredni segment podporowy (M_s) pierwszego przęsła, w którym jako pierwszym zostaje osiągnięta najpierw „lokalna" nośność krytyczna, a potem obliczeniowa nośność graniczna. Dla analizowanej w przykładzie belki, wykonanej z zimnogiętego profilu skrzynkowego Sk250x250x4 i obliczonej wg CPM, wykazano około 59-o procentowy wzrost „lokalnej" nośności krytycznej, co przełożyło się na prawie 10-o procentowy wzrost obliczeniowej nośności granicznej w stosunku do obliczeń wg EC-3.

Zastosowanie dokładniejszego modelu obliczeniowego pozwala zatem na bardziej optymalne projektowanie konstrukcji cienkościennych, w którym „nieznane" zapasy nośności konstrukcji zastępuje się obiektywnymi miarami niezawodności.